DFT study of the coverage-dependent chemisorption of molecular H_2 on neutral cobalt dimers

Constantinos D. Zeinalipour-Yazdi

Kathleen Lonsdale Materials Chemistry, Department of Chemistry, University College London, London, WC1H 0AJ, UK

We have studied the coverage-dependent chemisorption of H_2 on neutral cobalt dimers and found that there is a linear decrease of the adsorption energy and the metal-metal bond strength as a function of adsorbate coordination (i.e., θ, coverage). At a coverage below $\theta < 0.4$ the chemisorption is dissociative without a precursor-mediated physisorbed state and at $0.4 < \theta < 1$ it is both molecular and dissociative with a ratio of 6:1. During H_2 chemisorption which is entirely side-on there is a very large quenching of the magnetic moment $\Delta\mu = 4.9\ \mu_B$ and a linear weakening of the metal-metal bond strength, given by calculated oscillator frequencies. We show that sub-nanometer cobalt clusters when exposed to H_2 have strong coverage-dependent properties useful for the development of very sensitive H_2-trace gas sensors in the sub-ppm range.

1 Introduction

The adsorption of molecular hydrogen (H_2) on metal clusters is of interest in several fields, among which trace-gas sensors, heterogeneous catalysis, metallurgy, photocatalysis and hydrogen storage [1-6]. The interaction of hydrogen with cobalt surfaces is of particular industrial importance due to the use of cobalt as a Fisher-Tropsch (F-T) catalyst, in which the dissociation of hydrogen is one of the critical mechanistic steps towards the subsequent hydrogenation of carbon into hydrocarbons[7-13]. It is also an important process in the development of novel materials for H_2-sensors, as small amounts of cobalt have been found to increase the sensitivity of potential materials for H_2-sensors[14] and for trace-H_2 detection [15-18]. There are several experimental studies of the reaction of H_2 and D_2 with extented cobalt

surfaces [19-21]. They find that the adsorption of H_2 is dissociative at temperatures as low as 90K and that defects and steps have the capability of multiple atomic hydrogen (H_a) chemisorption rather than molecular hydrogen adsorption [20]. The studies on hydrogen chemisorption on Co(0001) surfaces showed that the maximum hydrogen coverage is ~0.5ML and only after sputtering, a denser H-overlayer of 0.75 ML, is obtained [21]. In practically most reported cases [19-21] a H_2 molecule dissociates during the adsorption on cobalt surfaces and nanoparticles, where the H atoms bind at the three-fold (3f) hollow sites. A detailed STM and DFT study revealed that a denser H-(1x1) phase is found on Co nanoparticles deposited on copper surfaces in which step edges are important in activating the dissociation of H_2, through spillover from the copper substrate [20]. There are however, only a few DFT studies of H_2 adsorption on cobalt nano-clusters. The effect of nanocluster size on the adsorption energy trends was modelled for the chemisorption of H-atoms on neutral Co_n nanoclusters (n = 1, 2, 3, 4, 5), which found that H chemisorbs in a bridged configuration [22]. Furthermore, DFT calculations showed that the adsorption of 3 H-atoms diminished the magnetic properties cubooctahedral and icosahedral Co_{13} clusters [23]. Cobalt clusters exhibit high magnetic moments, for example, Co_2 and Rh_2 dimers have been reported to have unusually high magnetic anisotropy energies (MAE) of 30 meV and 50 meV, respectively [24]. In particular, bimetallic dimers (i.e., Pt–Ir, Os–Ru) dimers form stable vertical structures on graphene sheets at defect sites, with MAE greater than 60 meV, sufficient for room-temperature magneto-electronic applications [25]. Magnetization measurements on Co-doped MoS_2 showed that smaller cobalt clusters have higher magnetic moments than larger nanoparticles [26]. Therefore, the presence of high magnetic moments in small cobalt clusters such as Co_2 and the possibility of funtionalising them to graphene sheets[27], makes them ideal for the development of novel materials for H-sensors or other megneto-electronic apllications in nanotechnology. There have been a few recent reports that have applied bimetallic[28] (e.g. Pt/Pd supported on Al_2O_3) and monometallic (e.g. Pd supported on MnO_2 nanowalls[29] and tubular $TiO_{2[30]}$) NPs for hydrogen sensing to concentrations as low as 10 ppm with a response time of less than 1 s. However, ultra-sensitive H-sensor in the ppb-range are currently not available and therefore preliminary computational studies are necessary to understand the coverage-dependent adsorption properties of H_2 on well-defined metal nanoclusters where the amount can be quantitatively determined. In particular, we are interested to address whether (a) the chemisorption of H_2 is dissociative, dissociative via a molecular

precursor state or molecular, (b) if certain quantitatitve relationships can be derived that correlate the coverage to a physical property, (c) what structural and infrared spectroscopic effects result due to the adsorption and (d) the degree of magnetic quenching that occurs to Co_2 during H_2 adsorption. We address these questions by performing unrestricted hybrid-DFT calculations of the adsorption of H_2 on the 5 low lying spin-states of $Co_2(H_2)_n$, where n = 1 to 11. We then present the equilibrium structures of the most stable structure among the five low lying spin-states of $Co_2(H_2)_n$ where n = 1 to 7. Then we present the adsorption energy and the vibrational frequency for the metal-metal (M-M) bond, as a function of H_2 coverage. In the last section of this paper we present how the magnetic properties of $Co_2(H_2)_n$ changes as a function of coverage and two structure-property-relationships (SPR) are derived from the computational data.

2 Computational methods

Unrestricted hybrid-DFT calculations were performed in Gaussian 03 and 09 [31], with the Becke three-parameter hybrid exchange functional[15] combined with the Lee-Yang-Parr non-local correlation functional[32], abbreviated as UB3LYP. The wavefunctions of the metal were described by the Stevens/Basch/Krauss Effective Core Potential (ECP) triple-split basis (CEP-121G). [33-35] Only functions that correspond to the spherical version (5d, 7f) of this basis set were included in the calculations to avoid linear dependencies observed in Cartesian basis sets (6d, 10f). Therefore all computations were performed using the UB3LYP/CEP-121G(Co),aug-cc-pVTZ(H) method (unless otherwise noted) as the basis-set-superposition-error (BSSE) corrected adsorption energies for this system differed by only 0.5 kcal/mol from the non-BSSE corrected adsorption energies. The second-order partial derivatives matrix (Hessian) was evaluated analytically at every optimization step. The SCF convergence criteria for the RMS density matrix and the total energy were set to 10^{-8} Hr/bohr and 10^{-6} Hr, respectively. The average free energy of adsorption per H_2 ($\Delta G^{\emptyset}{}_{H2}$) was calculated based on the following equation,

$$\Delta G^{\emptyset}{}_{H_2} = (G^{\emptyset}_{Co_2(H_2)_n} - G^{\emptyset}_{Co_2} - n \cdot G^{\emptyset}_{H_2})/n \quad (1)$$

,where $G^{\emptyset}_{Co_2(H_2)_n}$, $G^{\emptyset}_{Co_2}$ and $G^{\emptyset}_{H_2}$ are the Gibbs free energies of the cobalt hydrite complex, cobalt dimer and molecular hydrogen, at P = 1 atm and T = 298.15 K and n the number of H_2 molecules bound to the cluster. The adsorbate coverage (θ) was defined based on the cluster-adsorbate model that had the largest number of adsorbed H_2 given by,

$$\theta = n/7 \quad (2)$$

Therefore the term 'coverage' is only mentioned loosely in this paper and is not a strict 'surface coverage' but rather the 'degree of H_2-coordination' to the metal cluster. Spin contamination $<S^2>$ was checked for the $Co_2(H_2)_n$ complexes that had low lying spin states for their ground state and it was found to be negligible.

3 Results and Discussion

3.1 Hydrogen chemisorption on Co_2

Computational study of the adsorbate coverage-dependent properties of catalysts and materials is still a challenge as there are currently not any implemented algorithms in modelling softwares that can make a priori accurate prediction for the initial configuration of multiple adsorbates on clusters and surfaces. The common assumption is to place one adsorbate per surface metal atom in an end-on configuration, which works well for most extended surfaces, based on LEED studies. However, for transition metal (TM) clusters that have a high degree of unsaturation and therefore can accommodate multiple adsorbates, the single adsorbate configuration is always adequate. We have recently reported two simple algorithms (i) the domino algorithm and (b) the minimum energy algorithm that were applied to obtain the initial structure of carbon monoxide (CO) adsorbates on a Pd_{38} NP at high adsorbate coverages [36]. It was shown that at high coverages the domino algorithm that initially binds adsorbates at end-on positions at a distance that corresponds to physisorption, yields optimised structures for which the IR spectra are in better agreement with Diffuse Reflectance Infrared Fourier-Transform Spectra (DRIFTS), obtained over SiO_2 supported Pd-NPs. Contrary the minimum energy algorithm did not reproduce experimental DRIFTS spectra although both algorithms at $\theta = 1$ had the same average adsorption energy for CO for two completely different surface adsorbate structures, the first being an all-hollow CO configuration, whereas the later having three types of adsorbates (i.e., end-on, bridge, hollow) [36]. Therefore, in this paper we have applied a modified version of domino algorithm, which had the following steps: (i) The H_2 are placed equidistant in their molecularly bound state at a distance of 1.1 Å from each cobalt atom, with respect to their centre-of-mass, in a side-on configuration, (ii) the distance between the cobalt atoms was initially set to the optimized bond length of the bare Co_2 with a spin multiplicity (s.m.) of 1 (iii) standard stereochemical configurations (i.e., linear, trigonal, tetrahedral, trigonal

bipyramidal and octahedral) were applied at the metal centers to determine the initial configurations of H_2 with respect to Co_2. These structures are shown on the left side of Fig. 1 whereas the optimised structures are shown on the right. Note that for **$2H_2$** a linear configuration did not converge whereas a zig-zag structure converged and (iv) the appearance of dissociated hydrogen (i.e., H) species was alternated between initial structures, as bridge-bound H was found to be stable on Co_n nanoclusters, where n = 1 to 5 [22] and in this study for Co_2. For the complex with the highest saturation in H_2, $Co_2(H_2)_7$, the geometry of each cobalt atom was tetrahedral with a maximum of 3 coordinated H_2 molecules and 1 bridge H-atom. This structure has similar features as the structure of $[Co_2X_3L]X.nH_2O$ where X = Cl or Br and L = (4,5-dimethyl-3-pyrazolyl)aldazine where IR and electronic spectra showed that it is indeed tetrahedral with 2 bridge-bound ligands [37]. For the complexes that form due to scission of the M-M bond, e.g. $Co(H_2)_5$, there was a maximum of 5 coordinated H_2 molecule. We notice that at low-H_2 coverage (i.e., **$2H_2$** and **$3H_2$**), the chemisorption of H_2 is dissociative with absence of a precursor-mediated physisorbed state. In contrast, at higher coverage (i.e., **$4H_2$**, **$5H_2$**, **$6H_2$**, **$7H_2$**) H_2 adsorbs mostly molecularly with an entire side-on configuration, until θ became 1 which corresponds to a coordination of 6 H_2 and two b-H atoms. We note that the complexation of H_2 with Co_2 is stabilised by two bridging ligands (b-H) at high coverage, which prohibit the scission of the M-M bond by the formation of two three-center bonds (M-bH-M). The dissociation of Co_2 would cause problems to a sensor or a functionalised opto-electronic material with respect to the accurate amount of H_2 that can be chemisorbed at full coverage. However, we find that after the formation of the bridge-H bond the cohesive strength between the two metals is rather large, and that adsorption-induced scission is unlikely at standard temperature and pressure.

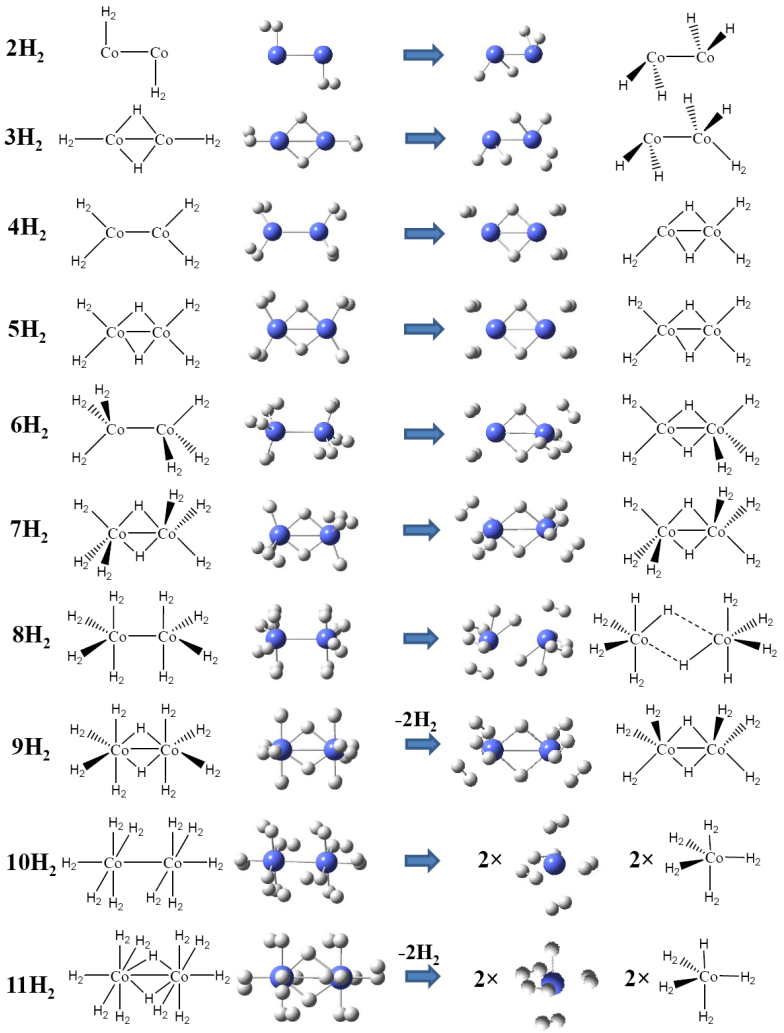

Fig. 1. Initial (left column) and optimized (right column) structures of the various $Co_2(H_2)_n$ configurations that have been examined at the UB3LYP/CEP-121G(Co),aug-cc-pVTZ(H) level of theory. Note that during the optimisation certain weakly bound H_2 desorb and in some cases there is a scission of the M-M bond in other cases.

Analysis of the structural features in the optimized H_2/cluster systems presented in Fig. 1 revealed the following qualitative observations: i) at low coverage ($\theta < 0.4$) the concentration of atomically adsorbed hydrogen is higher than the molecularly adsorbed species due to preference for dissociative adsorption, (ii) at higher coverage ($0.4 < \theta < 1$) the concentration of molecularly adsorbed hydrogen significantly exceeds that of atomically adsorbed species, (iii) each cobalt atom in the dimer can adsorb up to 3 molecular hydrogens and one bridged H, (iv) on an isolated cobalt atom there can be an adsorption of 5 molecular hydrogens, (v) high pressures of H_2 cause disruption of the metal-metal bond (i.e., **$8H_2$**, **$10H_2$** and **$11H_2$**), desorption of molecular hydrogen

(i.e. **$9H_2$** and **$11H_2$**) or both (i.e. **$11H_2$**) and (vi) molecular H_2 is adsorbed in all cases side-on with complete absence of an end-on configuration, in contrast to what has been found for the adsorption of H_2 on anions. CCSD(T)/aug-cc-pVTZ//CCSD/6-311++G(d,p) calculations for the adsorption of multiple H_2 on anions e.g. F^-, Cl^-, Br^-, OH^-, NH_2^-, NO_2^-, CN^- and ClO, showed that the stable adsorption configuration is primarily end-on[38]. There the number of coordinated H_2 molecules ranged between 12-20, indicative that the end-on configuration can accommodate a larger number of adsorbates, a useful feature in the design of H-storage materials that are based on anionic adsorption sites on functionalised materials.

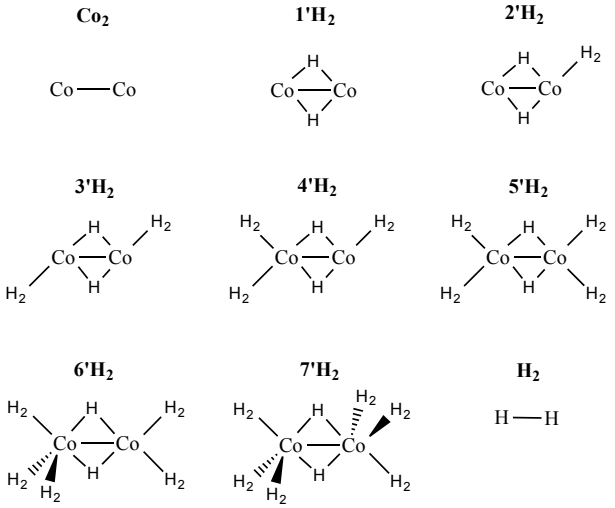

Fig. 2. Molecular structures and labels of the homologous series of cobalt hydrite, $Co_2(H_2)_n$ clusters, where n = 1 to 7.

In the following section the cobalt hydrite with the highest H_2 coverage (i.e., **$7'H_2$**) was further studied to understand the coverage dependent-properties of H_2 on Co_2. This particular structure, **$7'H_2$** shown in Fig. 2 was suitable to gradually decrease the number of chemisorbed H_2 without perturbing the other bonds within the molecular complex.

3.2 Coverage-dependent SPR for H_2 chemisorption on Co_2

Linear-SPR of the coverage-dependent adsorption energy of closed-shell molecules on NPs are mostly not observed, as there are usually a multitude of various adsorption configurations, each of different overall bonding strength. We have however shown that certain linear-SPR exist for the adsorption energy of CO on Rh_4 [39; 40] and Pd_4 [36] clusters which were applied as model systems to explain the coverage-dependent adsorption characteristics of

CO on transition-metal nanoparticles (TM-NPs). There the repulsive adsorbate-absorbate (A-A) and adsorbate-metal-adsorbate (A-M-A) repulsions caused a gradual weakening on the adsorbate-metal (A-M) bond [41]. Similarly in this study we have obtained certain linear-SPR for the coverage-dependent adsorption of H_2 on a cobalt dimer, which show a gradual linear weakening of the A-M bond as a function of θ. We note that SPR reported here are exceptionally linear, based on their R^2 values, which were 0.98 and 0.95, for the adsorption free energy and the oscillator frequencies graphs shown in Figure 3a and 3b, respectively. The exact functional form of both lines is a weakly sigmoidal curve. We interpret this weak non-linearity to the addition of more functions to the calculation as the coverage increases, as a result of BSSE, the absolute value of the BSSE was calculated to be of the order of 0.5 kcal/mol and therefore BSSE has been omitted for calculating the adsorption energies presented in Table 1. In particular, for the cobalt hydrites shown in Fig. 2 we have tabulated in Table 1 the average Gibbs free energy of H_2 adsorption ($\Delta G^{\emptyset}{}_{H_2}$), the oscillator frequency ($\nu_{M\text{-}M}$), the bond length ($r_{M\text{-}M}$) and the spin-only magnetic moment (μ_{so}) as a function of H_2 coverage (θ).

Table 1 Average Gibbs free energy of H_2 adsorption ($\Delta G^{\emptyset}{}_{H_2}$) per H_2, Raman oscillator frequency ($\nu_{M\text{-}M}$), bond length ($r_{M\text{-}M}$), spin multiplicity (s.m.), spin-orbit magnetic moment (μ_{so}) and point group (p.g.) as a function of H_2 coverage (θ) for Co_2, at the UB3LYP/CEP-121G(Co), aug-cc-pVTZ(H) level of theory.

Label	**♯ H_2**	**θ**	**ΔG_{ads} (kcal/mol)**	**$\nu_{M\text{-}M}$ (cm^{-1})**	**$r_{M\text{-}M}$ (Å)**	**s.m.**	**μ_{so} (μ_B)**	**p.g.**
Co_2	0	0.00	0	398	2.083	5	4.90	D_{infh}
1'H_2	1[1]	0.14	-25.1	329	2.265	5	4.90	D_{2h}
2'H_2	2	0.29	-20.8	308	2.264	1	0.00	C_1
3'H_2	3	0.43	-17.9	288	2.369	5	4.90	C_{2h}
4'H_2	4	0.57	-15.6	279	2.360	5	4.90	C_1
5'H_2	5	0.71	-14.0	273	2.437	3	2.83	D_{2h}
6'H_2	6	0.86	-11.5	266	2.419	3	2.83	C_s
7'H_2	7	1.00	-8.5	251	2.457	1	0.00	C_{2h}
H_2	-	-	-	(4418)[3]	(0.743)	1	0.00	D_{infh}

[1] one more envelope like structure found 0.01 Hr higher in energy
[2] A higher energy C_{2V} structure was also found in which H_2 are in eclipsed Newman configuration
[3] Values in parenthesis correspond to calculated properties for H_2

Fig. 3a shows the Gibbs free energy of adsorption of H_2 per H_2 ($\Delta G^{\emptyset}{}_{H2}$) as function of θ. Interestingly we observe that $\Delta G^{\emptyset}{}_{H_2}$ from -25.1 kcal/mol at θ = 0 becomes -8.5 kcal/mol at θ = 1. This corresponds to a four-fold decrease of the exothermicity of the adsorption energy by ΔΔE = 16.6 kcal/mol per H_2 which is rather large when compared to the adsorption of other closed shell molecules, such as carbon monoxide (CO). With identical computational methods we found in an earlier study that the low- to high-θ adsorption energy difference for CO bound to an Rh_4 cluster corresponds to ΔΔE = 13 kcal/mol. [41] In another study on a Pd_{38} NP[36] we find a decrease of the exothermicity of ΔΔE = 10 kcal/mol which suggests that there is also a cluster-size effect for the low-θ to high-θ adsorption energy difference. It is therefore apparent that the 16.6 kcal/mol ΔΔE found is an upper limit for the low- to high-θ decrease for the adsorption energy of H_2, compared to that of larger cobalt NPs. The equation that describes this linear-SPR for the coverage-dependent adsorption energy as a function of H_2 coverage is given by

$$\Delta G^{\emptyset}{}_{H_2}(kcal/mol) = 18.1 \cdot \theta - 24 \qquad (3)$$

This equation although specific for the particular molecular system can be implemented in an approximate way in kinetic models to take into account the coverage-dependent decrease of the adsorption energy of H_2 on small cobalt clusters.

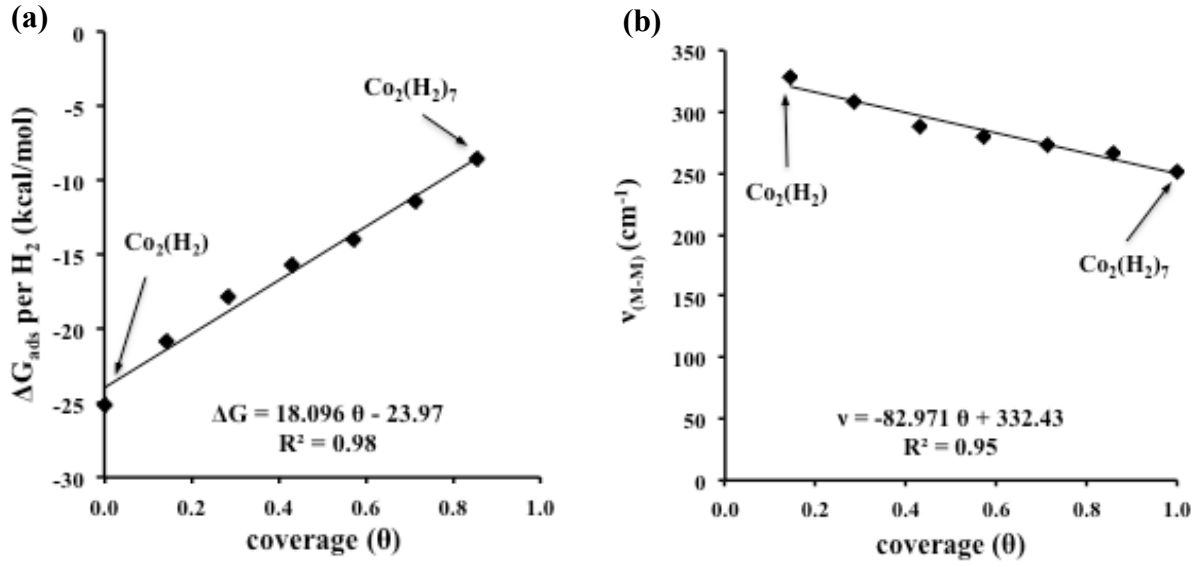

Fig. 3. (a) Free energy of adsorption per H_2 (b) and Raman shift of M-M stretching frequency as a function of coverage calculated at the UB3LYP/CEP-121G(Co),aug-cc-pVTZ(H) level of theory. θ is defined in Eqn. 2. Solid line is a linear regression fit to the datapoints.

In Fig. 3b we present Raman shift for the oscillator frequencies of H-H as a function of θ. A similar near-linear sigmoidal curve is observed, as in the case of $\Delta G^{\emptyset}{}_{H_2}$, although with a negative slope. This is expected as the adsorption strength of every additional H_2-Co_2 bond formed gradually weakens the M-M bond strengh as a function of θ, and a smaller bond strength results in smaller oscillator frequencies according to the harmonic oscillator model. We find a considerably large decrease of the oscillator frequency (49 cm^{-1}) is considerably large which should be measurable by vibrational spectroscopic methods such as ATR and DRIFTS. The equation that describes this linear-SPR for the coverage-dependent IR frequency of the M-M bond as a function of θ is given by

$$v_{M-M}(cm^{-1}) = -82.9 \cdot \theta + 332 \quad (4)$$

This equation can be applied to estimate the number of H_2 molecules chemisorbed to Co_2 from IR spectra. Furthermore, based on the range of IR values tabulated in Table 1 we estimate that the sensor/detector material would have to be sensitive in the far-IR region between 250-330 cm^{-1} where coverage-dependent IR shifts during H_2 adsorption are measureable.

A simple electrostatic interpretation of the the linear-SPR found by Eqn. 4 in cobalt hydrite complexes of Cl and Br where the M-M distance in the Br-complex is smaller than in Cl-complex, due to the larger electronegativity of chloride.[42] This suggests that the formation of polarised covalent bonds between Co-halogens due to π-backdonation into the lowest-unoccupied orbital of the halogen, decreases the availability of electron density in the bonding orbitals of Co_2, causing decrease if the distance between the Co atoms. In analogy we can interpret the H_2-coverage dependent increase of the M-M bond, as a result of gradual loss of electron density belonging to filled π-orbitals at the dimer bond, into the empty anti-bonding orbitals of H_2. Both trends can be explained in the context of adsorbate-induced charge transfer from the dimer into the anti-bonding orbitals of adsorbates. It is insightful to encounter again that the coverage-dependent adsorption energy is a function of availability of filled bonding states of the metal clusters into empty states or the adsorbates which was also found to be the main electrostatic interpretation of bond formation for the case of CO adsorption on Rh[41] and Pd[36] clusters.

3.3 Magnetic properties as function of coverage

Stern-Gerlach deflection measurements have shown that cobalt clusters in the range Co_{65} to Co_{215} exhibit super-paramagnetic behaviour, with an average magnetic moment of 2.24 ± 0.14 μ_B per Co atom (at 300 K)[43]. This suggests that the reduced dimensionality and increased surface-to-volume ratio of clusters leads to enhanced magnetism which is quenched by the chemisorption of closed shell molecules such as hydrogen, as we show in Fig. 4b and as this has been previously shown for the adsorption of Co on Rh_n (n = 3-13) clusters. Currently there are not any reported examples of Co_2/H_2-sensors in the literature, although there is a very sensitive electrochemical sensor for H_2O_2 which is based on a trimeric Co_2-Fe clusters coordinated to 6CN groups, forming $Co_2^{II}Fe^{II}(CN)_6$.[44] This sensor material was found to have an unusually low detection limit 6.25×10^{-8} M when the complex was embedded in a glossy carbon electron due to electron transfer of the Co_2 dimer to H_2O_2. It also has a linear response to concentrations up to 1.1×10^{-3} M, based on cyclic voltammograms. Therefore analogous sensor materials for H_2 could be developed via functionalization of Co_2 to glossy carbon electrodes.

In Table 1 the Gibbs free energies of H_2 adsorption of the most stable spin multiplicity at each hydrogen coverage is tabulated. At $\theta = 0$ the neutral cobalt dimer has an s.m. of 5 which corresponds spin-only magnetic moment (μ_{SO}) of 4.9 μ_B per Co atom. With the only exception of **2'H$_2$** there is a constant decrease of the magnetic moment of the cobalt cluster as a function of the number of H_2 molecules adsorbed to it shown in Fig. 4b. At large coverage $\theta > 0.5$ the magnetic moment was found to be significantly lower, 2.83 μ_B per Co atom and at full coverage there is a complete quenching of the magnetic moment of Co_2. This is a very abrupt change in the magnetic moment of $\Delta\mu = 4.9$ which could be an interesting property for its application in trace gas sensor of H_2 that operate in the ppb range as the magnetic response measurements could be titrated on the basis of Co_2 specific surface density.

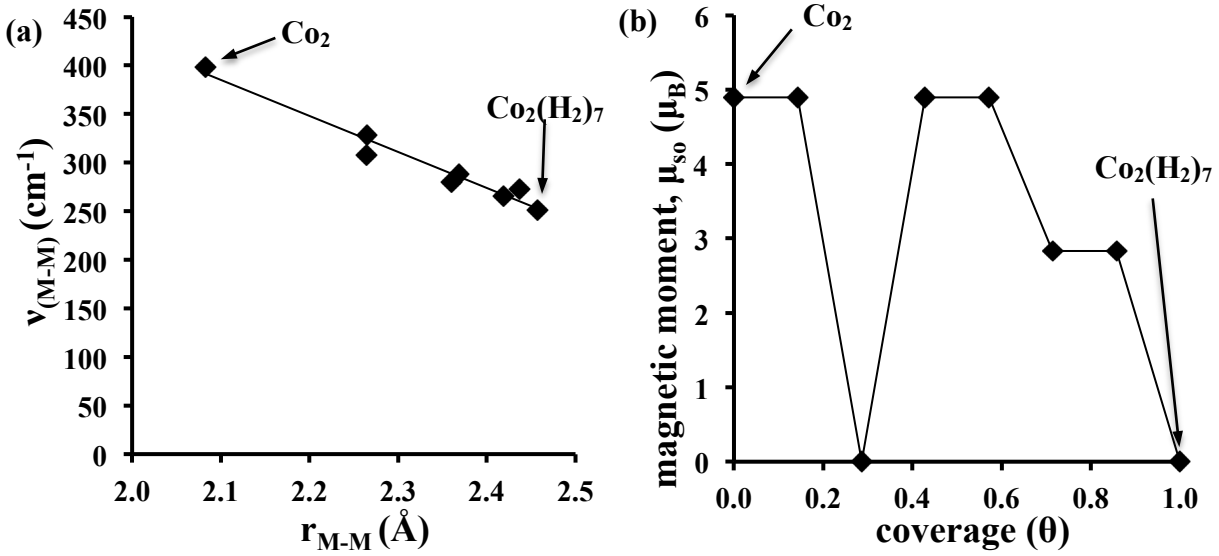

Fig. 4. (a) Vibrational frequency (ν_{M-M}) of M-M bond as a function of its length (r_{M-M}) (b) spin-only magnetic moment as a function of θ calculated at the UB3LYP/CEP-121G(Co),aug-cc-pVTZ(H) level of theory. Coverage defined in Eqn. 2. Solid line is a linear regression fit.

One aspect that is important during the reaction of H_2 with small clusters of cobalt is that, the Co_2-H_2 bond strength, may exceed the interactions between the cobalt atoms in Co_2, resulting in scission of the M-M bond. This has been observed for the reaction of O_2 with Co_2 in rare gas matrices using IR spectroscopy. [45] This would be a disadvantage in certain flow systems as it would cause contamination of the feedstream with cobalt and gradual degradation of the sensor material. In Fig. 4a we show that although the adsorption of H_2 causes a significant weakening of the M-M bond, seen by a 16% increase of the bond length, and a decrease of the vibrational frequency by 45 %, there is still a significant strength of the M-M bond based on the vibrational frequency of 250 cm^{-1} that the M-M bond has at θ =1. Furthermore, the optimisation results for **$10H_2$** and **$11H_2$** where a scission of the M-M is observed, should be regarded to be a result of starting with an initial structure, that due to the high density of the H_2 molecules, has significant degree of internal energy and therefore undergoes breaking of the M-M bond. Such conditions may only be accessible for H_2 at very high-pressures, and therefore at ambient pressures, such as those found in ambient-pressure flow systems we do not expect scission of the M-M bond. The above results suggest that a H_2 sensor system based on Co_2, is possible, and the existence of the linear SPR between IR frequency of the cobalt-cobalt bond as a function of H_2 coverage can be applied to calibrate the H_2-sensor in the ppb range, as current H_2-sensor materials are only available in the ppm range. Another detection method less sensitive maybe based on the

quenching of the magnetic moment of the Co_2 clusters upon H_2 adsorption. A recent DFT study showed that magnetic moment of two PAH-supported Co atoms is smaller than that of the end-on adsorbed dimer[27], therefore our calculations show that a sensor material based on Co_2 rather than Co would be more sensitive. These rather technical aspects will become relevant for the design of functional conductive paramagnetic materials functionalised with Co_2, which was recently shown to bind to graphene while preserving it's magnetic properties [46].

4 Summary

We have studied via hybrid DFT calculations the coverage-dependent chemisorption of H_2 on neutral cobalt dimers as model systems to understand the coverage-dependent structural, infrared, energetic and magnetic properties. Our simulations show that the adsorption of H_2 at coverages below 0.4 is dissociative without a precursor-mediated physisorbed state, whereas at coverages above 0.4 it is molecular/dissociative with a ratio of 6:1. There is a significant coverage-dependent quenching of the magnetic moment of the dimer by 4.9 bohr magnetons per Co with a concurrent four-fold linear decrease of the adsorption energy of H_2 as a function of hydrogen coverage. This is accompanied by a linear weakening of the M-M bond strength, as calculated from Raman oscillator frequencies. The good linearity found between the IR oscillator frequencies and the H_2 coverage could be a novel property for the design of novel H_2-sensor materials, based on cobalt dimers functionalised to paramagnetic/conductive materials.

Acknowledgements

C.D.Z-Y. acknowledges the use of the UCL Legion High Performance Computing Facility (Legion@UCL), and associated support services, in the completion of this work and funding from EPSRC EP/L026317/1.

Corresponding Author

*E-mail: c.zeinalipour-yazdi@ucl.ac.uk. Tel: +44 207-679-0312

References:

[1] I. Swart, P. Gruene, A. Fielicke, G. Meijer, B.M. Weckhuysen, F.M.F. de Groot, Phys. Chem. Chem. Phys. 10 (2008) 5743–5745.

[2] S. Shevlin, Z. Guo, J. Phys. Chem. C 117 (2013) 10883-10891.

[3] C. Shang, M. Bououdina, Y. Song, Z. Guo, Int. J. Hydrogen Energy 29 (2004) 73-80.
[4] D.G.H. Hetterscheid, C.J.M. van der Ham, O. Diaz-Morales, M.W.G.M. Verhoeven, A. Longo, D. Banerjee, J.W. Niemantsverdriet, J.N.H. Reek, M.C. Feiterse, Phys. Chem. Chem. Phys. 18 (2016) 10931-10940.
[5] A. Fernandoa, C.M. Aikens, Phys. Chem. Chem. Phys. 17 (2015) 32443-32454.
[6] B.B. Xiao, X.B. Jiang, Q. Jiang, Phys. Chem. Chem. Phys. 18 (2016) 14234-14243.
[7] I.A.W. Filot, R.A. van Santen, E.J.M. Hensen, Catal. Sci. Technol. 4 (2014) 3129-3140.
[8] R.A. van Santen, M. Ghouri, E.M.J. Hensen, Phys. Chem. Chem. Phys. 16 (2014) 10041-10058.
[9] R.A. van Santen, A.J. Markvoort, I.A.W. Filot, M.M. Ghouri, E.J.M. Hensen, Phys. Chem. Chem. Phys. 15 (2013) 17038-17063
[10] R.A. van Santen, A.J. Markvoort, M.M. Ghouri, P.A.J. Hilbers, E.J.M. Hensen, J. Phys. Chem. C 117 (2013) 4488-4504.
[11] I.M. Ciobîcă, P. van Helden, R.A. van Santen, Surf. Sci. 653 (2016) 82-87.
[12] C.J. Weststrate, P.v. Helden, J.v.d. Loosdrecht, J.W. Niemantsverdriet, Surf. Sci. 648 (2016) 60-66.
[13] J. Yang, V. Frøseth, D. Chen, A. Holmen, Surf. Sci. 648 (2016) 67-73.
[14] L.P. Oleksenko, N.P. Maksymovych, A.I. Buvailo, I.P. Matushko, N. Dollahon, Sensor. Actuat. B - Chem. 174 (2012) 39-44.
[15] A.D. Becke, J. Chem. Phys. 98 (1993) 5648.
[16] A. Othonos, C. Christofides, Appl. Phys. Lett. 82 (2003) 904-906.
[17] C. Christofides, A. Mandelis, J. Appl. Phys. 66 (1989) 3986-3992.
[18] C. Christofides, A. Mandelis, J. Appl. Phys. (1990) R1-R30.
[19] M.E. Bridge, C.M. Comrie, R.M. Lambert, J. Catal. 58 (1979) 28-33.
[20] E.A. Lewis, D. Le, C.J. Murphy, A.D. Jewell, M.F.G. Mattera, M.L. Liriano, T.S. Rahman, E.C.H. Sykes, J. Phys. Chem. C 116 (2012) 25868-25873.
[21] P. van Helden, J.-A. van den Berg, C. Westrate, ACS Catal. 2 (20-12) 1097-1107.
[22] F. Buendia, M.R. Beltran, Comput. Theor. Chem. 1021 (2013) 183-190.
[23] Š. Pick, H. Dreyssé, Surf. Sci. 460 (2000) 153-161.
[24] T.O. Strandeberg, C.M. Canali, A.H. MacDonald, Nature Mat. 6 (2007) 648-651.
[25] J. Hu, R. Wu, Nano Lett. 14 (2014) 1853–1858.
[26] Z. Xiang, Z. Zhang, X. Xu, Q. Zhang, Q. Wanga, C. Yuanc, Phys. Chem. Chem. Phys. 17 (2015) 15822-15828.
[27] M. Mahmoodinia, P.-O. Åstrand, D. Chen, J. Phys. Chem. C 119 (2015) 24425–24438.
[28] K. Hassan, A.S.M. Iftekhar Uddin, G.-S. Chung, Sensor Actuat B-Chem 234 (2016).
[29] A. Sanger, A. Kumar, A. Kumar, R. Chandra, Sensors and Actuat B-Chem 29 (2016) 8–14.
[30] J. Moon, H.-P. Hedman, M. Kemell, A. Tuominen, R. Punkkinen, Sensors Actuat B-Chem 222 (2016) 190–197.
[31] M.J. Frisch *et al.*, GAUSSIAN03, Gaussian Inc, Wallingford CT, 2004.
[32] C. Lee, W. Yang, R.G. Parr, Phys. Rev. B 37 (1988) 785.
[33] T.R. Cundari, W.J. Stevens, J. Chem. Phys. 98 (1993) 5555.
[34] W. Stevens, H. Basch, J. Krauss, J. Chem. Phys. 81 (1984) 6026.
[35] W.J. Stevens, M. Krauss, H. Basch, P.G. Jasien, Can. J. Chem. 70 (1992) 612.
[36] C.D. Zeinalipour-Yazdi, D.J. Willock, L. Thomas, K. Wilson, A.F. Lee, Surf. Sci. 646 (2016) 210-220.

[37] A. El-Dissouky, G.B. Mohamad, Inorg. Chim. Acta 162 (1989) 263-270.
[38] T.D. Della, C.H. Suresh, Phys. Chem. Chem. Phys. 18 (2016) 14588-14602.
[39] C.D. Zeinalipour-Yazdi, A.L. Cooksy, A.M. Efstathiou, J.Phys. Chem. C 111 (2007) 13872-13878.
[40] C.D. Zeinalipour-Yazdi, A.L. Cooksy, A.M. Efstathiou, Surf. Sci. 602 (2008) 1858-1862.
[41] C.D. Zeinalipour-Yazdi, R.A. van Santen, J. Phys. Chem. C 116 (2012) 8721-8730.
[42] D.M. Duggan, D.N. Hendrickson, Inorg. Chem. 4 (1975) 1944.
[43] D.C. Douglass, A.J. Cox, J.P. Bucher, L.A. Bloomfield, Phys. Rev. B 47 (1993) 12874.
[44] M.S. Lin, B.I. Jan, Electroanalysis 9 (1997) 340–344.
[45] D. Danset, L. Manceron, Phys . Chem. Chem. Phys. 7 (2005) 583-591.
[46] J. Hu, R. Wu, Nano Lett. 14 (2014) 1853-1858.